*e-Polymers* **2011**, no. 009 http://www.e-polymers.org
ISSN 1618-7229

# Shear degradation resistance of star poly(ethyleneimine) - polyacrylamides during elongational flow

*Ming Duan,[1] Shenwen Fang,[1] Liehui Zhang,[1*] Fuxiao Wang,[1] Peng Zhang,[1] Jian Zhang[2]*

[1*]State Key Laboratory of Oil/Gas Reservoir Geology and Exploitation, Southwest Petroleum University, Chengdu, Sichuan 610500, China; Fax number: +86-28-8303 - 2901; e-mail:fangwen1228@yahoo.com.cn.
[2]Beijing Research Center of China National Offshore Oil Corporation, Beijing 100027, China; e-mail:swpud317@163.com.

(Received: 21 April, 2010; published: 18 February, 2011)

***Abstract:*** An experimental study of the flow-induced scission behaviour of four star hydrolyzed polyacrylamides (HPMA) with different arms during planar elongational flow in a cross-slot flow cell is described. The results showed that the shear stability of linear HPAM in distilled water was not essentially different from star HPAM. Polymer scission was not observed in either system in a shear rate range from 20,000 to 100,000$s^{-1}$, which can be attributed to the strong polyelectrolyte behaviour of HPAM in distilled water. However, at the same shear rate, the star HPAMs exhibited superior shear stability in comparison to the linear HPAMs in aqueous solutions containing NaCl ($C_{NaCl}$=0.2-1.0%wt) and, in particular, the initial reduction rate of relative viscosity (*R*) decreased with the degree of branching of the HPAMs. In addition, it was found that the *R* of five HPAMs in NaCl aqueous solutions exhibited an exponential dependence on shear rate, in which the coefficient $C_1$ can be used to quantitatively evaluate shear stability. In star HPAM NaCl aqueous solutions, the increase of *R* with shear rate is very likely due to the decrease of the hydrodynamic radius ($R_h$) of these HPAMs, while the increase of *R* with NaCl concentrations can be attributed to the relatively low viscosity of these polymers at high NaCl concentrations.

## Introduction

Hydrolyzed polyacrylamide (HPAM) has been widely used as thickening agents in enhanced oil recovery (EOR) [1-3]. Adding a small amount of HPAM (1200-2000mg/L) in the injection water can significantly enhance its viscosity. Unfortunately, the viscosity of HPAM solution usually declines rapidly when continuously exposed to mechanical shearing action, either by strong mechanical stirring in the process of dissolution or by passing through capillary pores in the petroleum reservoirs, indicating a rapid breakdown of the polymer chains [4, 5]. The degradation of polymer chains is likely due to the scission of molecular entanglements as well as the breakage of individual molecules induced by the shear stresses associated with very high local shear rate [6]. Most HPAMs used in EOR are linear polyacrylamides (PAM). However, it has been reported by Kim et al, as early as in 1975, that grafted PAM (branched polymers) exhibited much better shear stability than linear PAM [7]. Moreover, it has been confirmed that attaching side chains to the polymeric backbone can effectively enhance the shear stability in turbulent flows, which can be

attributed to the sacrificial scission of the branches that leads to only a minor decrease of molecular weight [8, 9].

Amongst branched polymers, star PAM is particularly interesting because it possesses an elementary branching topology with multiple linear chains linked to a single core. In our previous work, we reported the synthesis of a novel class of star PAMs with different arms via photopolymerization [10]. In this paper, we report an experimental study of their shear stability during elongational flow and compare the results with those of linear HPAM.

## Results and discussion

During polymer stretching in a strong elongational flow, tensile stresses build up from chain ends toward chain centre until chain breakage occurs at the centre. In a steady, strong, elongational flow of a dilute solution, the cumulative stress along a linear polymer chain reaches its maximum at the chain centre ($\sigma_c$) [11-13]:

$$\sigma_c=\sigma_{max}=\xi b \dot{\varepsilon} N_l^{\,2}/2 \qquad (1)$$

In which $b$ is the stretched segment length, $\xi$ is the hydrodynamic drag coefficient of the beads and $N_l$ is the number of the stretched segments.

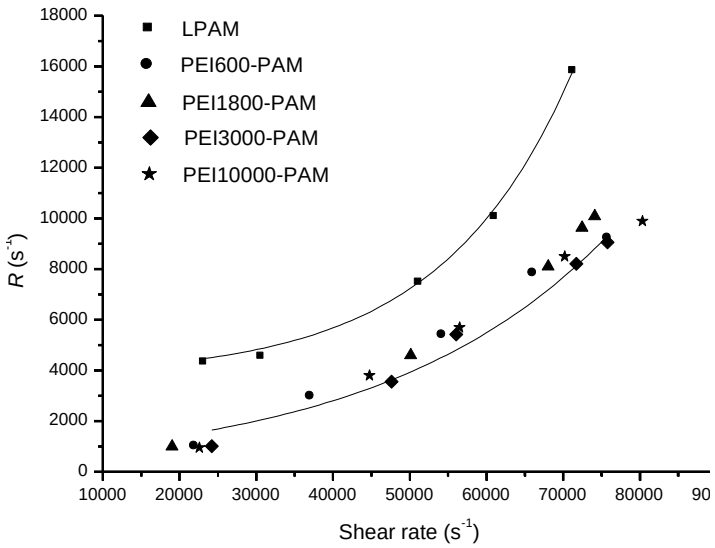


**Fig. 1.** *R* vs shear rate for different PAMs in distilled water.

Eqn.1 ($\sigma_{max} \propto N_l^{\,2}$, for linear polymers) has been extended by Xue et al [14] to describe the stress distribution in star polymers. They found that the maximum stress on a star polymer's arms followed $\sigma_{max} \propto N_s^2/n^2$, where $n$ is the number of arms the star polymer has and $N_s$ is the number of segments per arm. On the other hand, according to a theory called critical stress to fracture (CSF), chain scission occurs whenever the tensile stress ($\sigma$) in a segment exceeds the C-C single bond strength. The $\sigma_{max}$ in a star polymer chain is much smaller compared to a linear polymer of the same total molecular weight ($N_l = nN_S$). Consequently, the star polymer is more difficult to break and, in particular, the sacrificial scission of the branches would lead to only a small decrease in molecular weight in the case of $\sigma > \sigma_c$. In ref [14], the initial

scission rate $R$ was plotted as a function of the shear rate and the authors found an exponential relationship

$$R = C_1 \exp(C_2 \dot{\varepsilon}) \quad (2)$$

In EOR, viscosity is the most important property of a polymer solution. In this paper, relative viscosity was chosen to evaluate the scission behaviour of different star PAMs. Figure 1 shows the variation of the initial rate of reduction of relative viscosity ($R$) as a function of the shear rate for the five PAMs. All experimental data can be well fitted by an exponential function and the correlation coefficients were all >0.98. In particular, the $R$ of LPAM was much larger than for the PEI-PAMs. Thus the star PAMs had higher shear stability than LPAM. However, a difference in $R$ among the four PEI-PAMs was not obvious.

The values of $C_1$ and $C_2$ are shown in Table 1 for the five PAMs. All the $C_2$ values were pretty small and showed little difference, while the $C_1$ values were much larger and can reflect the differences in $R$ among the five samples. In particular, LPAM had the largest $C_1$ value while the $C_1$ values of the other four samples were similar.

**Tab. 1.** The values of $C_1$ and $C_2$ for five PAMs.

| | LPAM | PEI600-PAM | PEI1800-PAM | PEI3000-PAM | PEI10000-PAM |
|---|---|---|---|---|---|
| $C_1$ ($s^{-1}$) | 1432.89 | 490.21 | 489.31 | 489.17 | 488.55 |
| $C_2$ (s ) | 0.000039 | 0.000040 | 0.000042 | 0.000042 | 0.000040 |

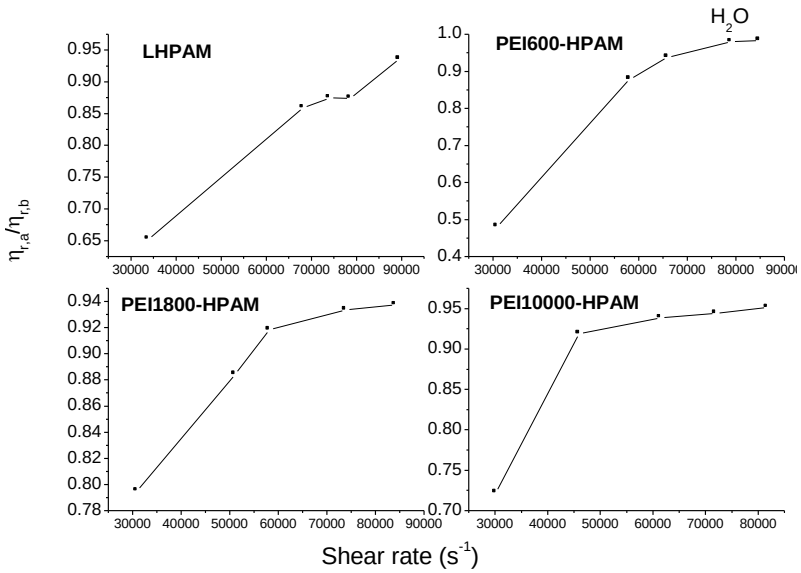


**Fig. 2.** $\eta_{r,a}/\eta_{r,b}$ vs shear rate for different HPAMs in water.

Figure 2 shows the $\eta_{r,a}/\eta_{r,b}$ - shear rate correlation for the four HPAMs in distilled water. Although all the $\eta_{r,a}/\eta_{r,b}$ were smaller than 1.0, the $\eta_{r,a}/\eta_{r,b}$ increased remarkably with the shear rate. These results were very different from the PAMs in distilled water. The size (hydrodynamic radius, $R_h$) distributions of PEI10000-HPAM before and after scission are shown in Figure 3. Essentially no variation was observed. Similarly, there were no changes in the intrinsic viscosities of different PEI-

HPAM observed before and after the scission experiments (Table 2). These results indicate that no breakage occurred in the HPAM polymer chains, which can be attributed to the strong polyelectrolyte behavior of HPAM in distilled water. For instance, HPAM (both linear and star HPAM) took an expanded conformation in dilute aqueous solutions as a result of net charges development in the domains of the polymer chain. In particular, the single polymer molecule can extend virtually to their maximum length in sufficiently diluted solutions. Consequently, the random intermolecular entanglements can be very serious and lead to the formation of a "network". The entanglements can be broken in an elongational flow and results in the decrease in $\eta_r$. The polymer chains that were released from a broken entanglement can extend along the elongation direction again as the shear rate increases. The polymer chains can become more extended, and the entanglements along the elongation direction can be easily recovered and the $\eta_{r,a}$ increased.

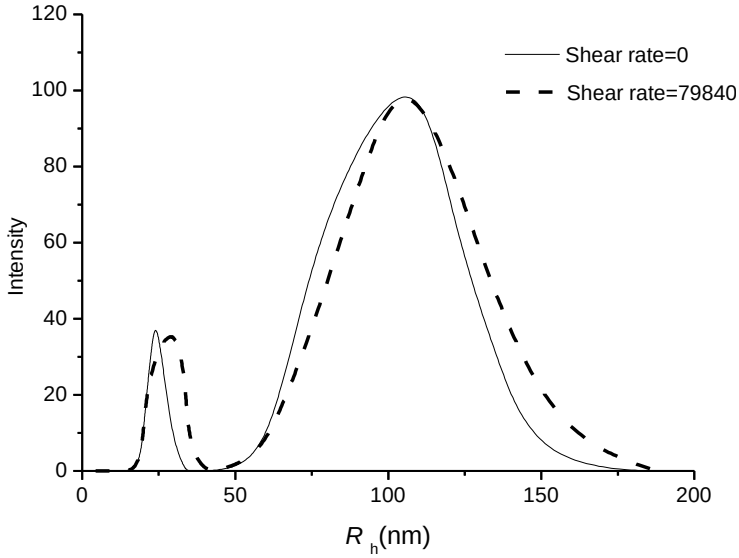


**Fig. 3.** Distributions of $R_h$ of the PEI10000-HPAM in 1.0% NaCl aqueous solution after scission experiment in distilled water.

**Tab. 2.** Intrinsic viscosities of PEI-HPAMs in 0.1mol/L NaCl before and after the scission experiment in distilled water.

| Sample | LHPAM | PEI600-HPAM | PEI1800-HPAM | PEI3000-HPAM | PEI1000-HPAM |
|---|---|---|---|---|---|
| $[\eta]_b$ (dL/g) | 12.90 | 11.91 | 11.46 | 11.03 | 10.28 |
| $[\eta]_a$ (dL/g) | 12.90 | 11.90 | 11.46 | 11.03 | 10.28 |

Figures 4-7 show the plots of $R$ vs shear rate for five HPAMs in aqueous solutions of different NaCl concentrations. At the same shear rate, $R$ decreased with the branching degree of HPAM. It was also found that Eqn.2 can be used to describe the behaviour of the five HPAMs in NaCl aqueous solutions. The $C_1$ and $C_2$ values are summarized in Tables 3 and Table 4, respectively. Similar to PAMs in distilled water, $C_1$ can be used to predict the viscosity shear stability of the different polymers.

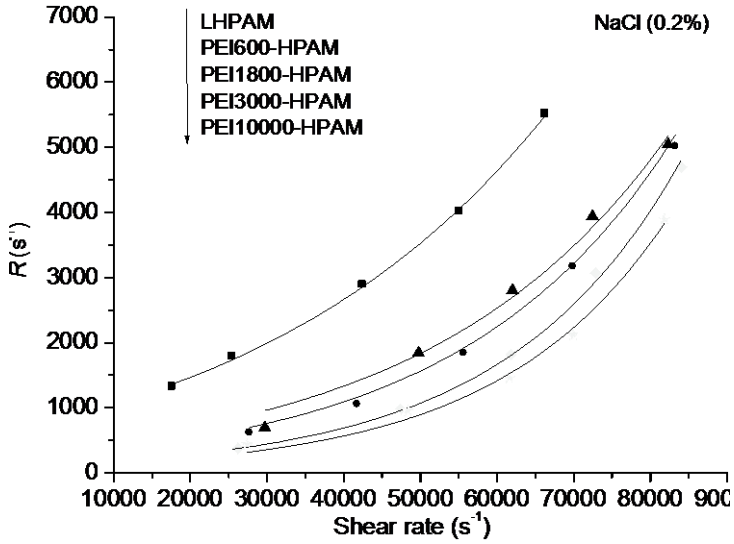


**Fig. 4.** *R* vs Shear rate for different HPAMs in 0.2% NaCl aqueous solution.

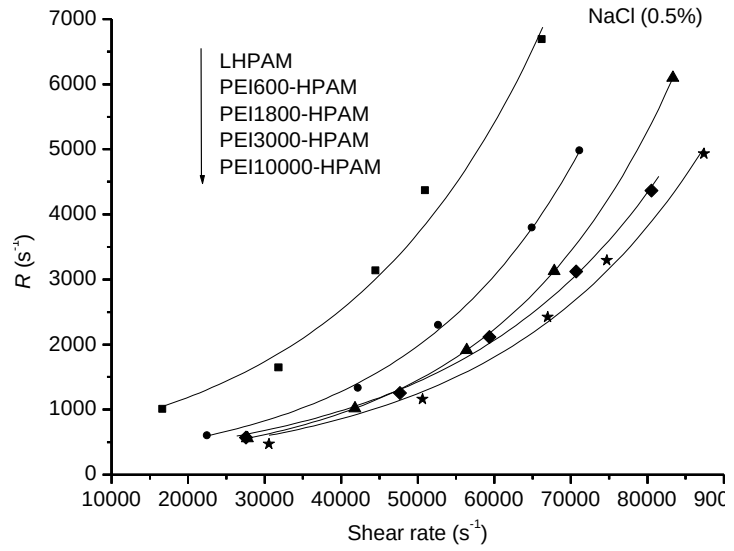


**Fig. 5.** *R* vs Shear rate for different HPAMs in 0.5% NaCl aqueous solution.

As shown in Figure 8 and Table 5, $R_h$ increased while $\Delta[\eta]$ decreased with the degree of branching of HPAM after the flow-induced scission experiment (shear rate ≈ 80,000$s^{-1}$). This explains why *R* decreased with the degree of branching of the HPAM.

For every HPAM, *R* increased with the shear rate (Figures 4-7), which can be attributed to the increase in scission of the arms from the polymer chain. $R_h$ distributions of the PEI10000-HPAM after the scission experiments in 1.0% NaCl aqueous solution are shown in Figure 9 for different shear rates. The lines dash a and b represent the peak positions of the complete arms obtained by arm cleavage [14] and of the original star HPAM, respectively. The low $R_h$ peak (dash a) area that corresponds to the arms that were cleaved increased with the shear rate, resulting in the decrease in $R_h$ average as shear rate increased.

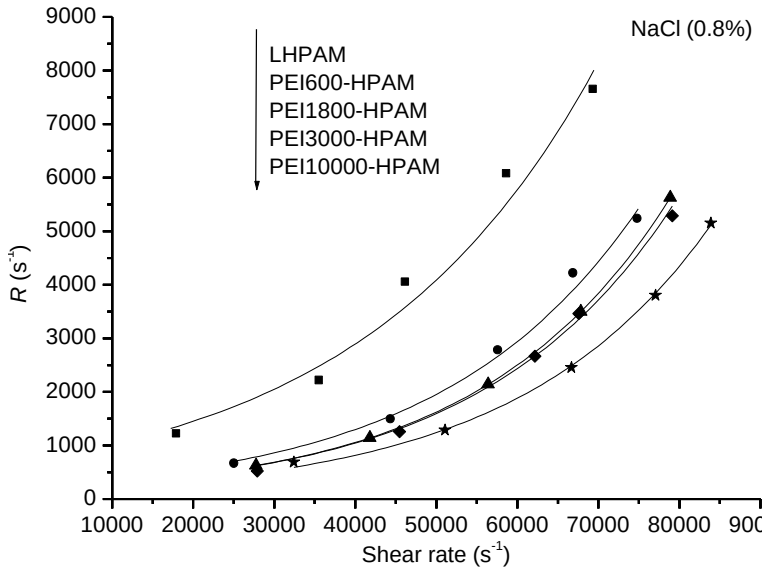


**Fig. 6.** *R* vs Shear rate for different HPAMs in 0.8% NaCl aqueous solution.

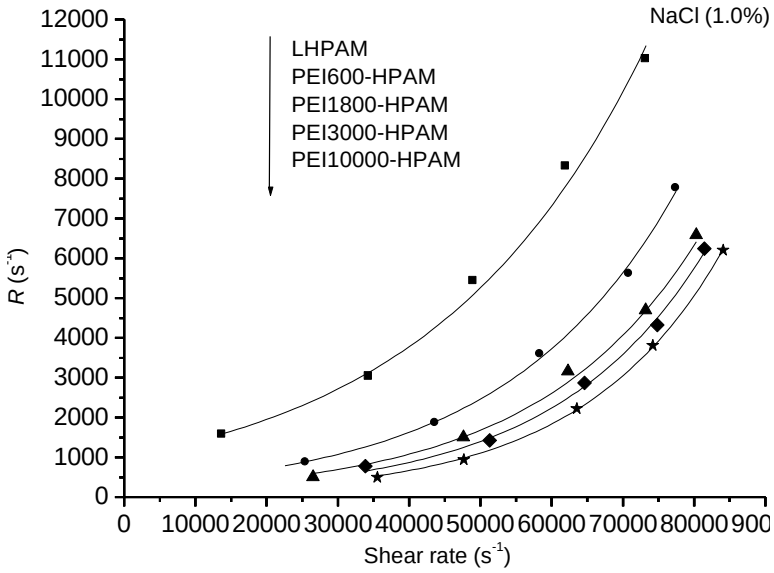


**Fig. 7.** *R* vs Shear rate for different HPAMs in 1.0% NaCl aqueous solution.

**Tab. 3.** The values of $C_1$ for five HPAMs ($s^{-1}$).

| $C_{NaCl}$(%wt) | LHPAM | PEI600-HPAM | PEI1800-HPAM | PEI3000-HPAM | PEI10000-HPAM |
|---|---|---|---|---|---|
| 0.2 | 580.77 | 164.37 | 158.43 | 129.99 | 119.67 |
| 0.5 | 600.55 | 182.56 | 169.40 | 150.91 | 136.01 |
| 0.8 | 646.53 | 223.44 | 189.73 | 173.78 | 152.75 |
| 1.0 | 819.87 | 300.51 | 204.26 | 180.60 | 158.01 |

**Tab. 4.** The values of $C_2$ for five HPAMs (s).

| $C_{NaCl}$(%wt) | LHPAM | PEI600-HPAM | PEI1800-HPAM | PEI3000-HPAM | PEI10000-HPAM |
|---|---|---|---|---|---|
| 0.2 | 0.000038 | 0.000043 | 0.000043 | 0.000042 | 0.000042 |
| 0.5 | 0.000037 | 0.000043 | 0.000043 | 0.000043 | 0.000042 |
| 0.8 | 0.000037 | 0.000043 | 0.000043 | 0.000044 | 0.000042 |
| 1.0 | 0.000037 | 0.000042 | 0.000043 | 0.000044 | 0.000044 |

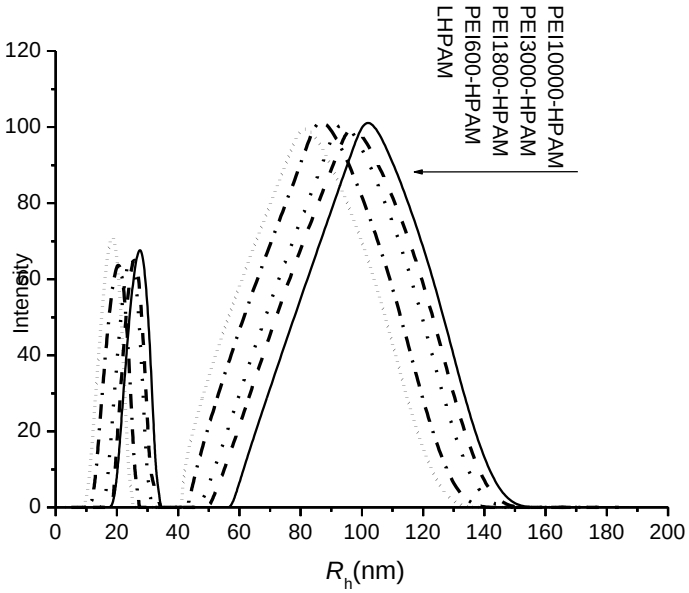


**Fig. 8.** Distributions of $R_h$ of five HPAMs in1.0% NaCl aqueous solution after scission experiment in 1.0% NaCl aqueous solution (shear rate ≈ 80,000$s^{-1}$).

**Tab. 5.** Intrinsic viscosities of PEI-HPAMs in 0.1mol/L before and after the scission experiment in 1.0% NaCl aqueous solution.

| Sample | LHPAM | PEI600-HPAM | PEI1800-HPAM | PEI3000-HPAM | PEI10000-HPAM |
|---|---|---|---|---|---|
| $[\eta]_b$ (dL/g) | 12.90 | 11.91 | 11.46 | 11.03 | 10.28 |
| $[\eta]_a$ (dL/g) | 9.76 | 9.95 | 9.87 | 9.68 | 9.15 |
| $\Delta[\eta]$(%) | 24.34 | 16.49 | 13.89 | 12.23 | 11.03 |

It was also found from Figures 4-7 that $R$ increased with NaCl concentration. As shown in Figure 10, this result cannot be completely attributed to the increase of scission of polymer chains. Particularly, at NaCl concentrations larger than 0.2%, the $R_h$ distributions of PEI10000-HPAM in 1.0% NaCl aqueous solution actually remained essentially unchanged after the scission experiments in various NaCl aqueous solutions (shear rate ≈ 80,000$s^{-1}$). The increase of $R$ with NaCl concentration may be due to the decrease of polymer viscosity $\eta_r$ as NaCl concentration increased.

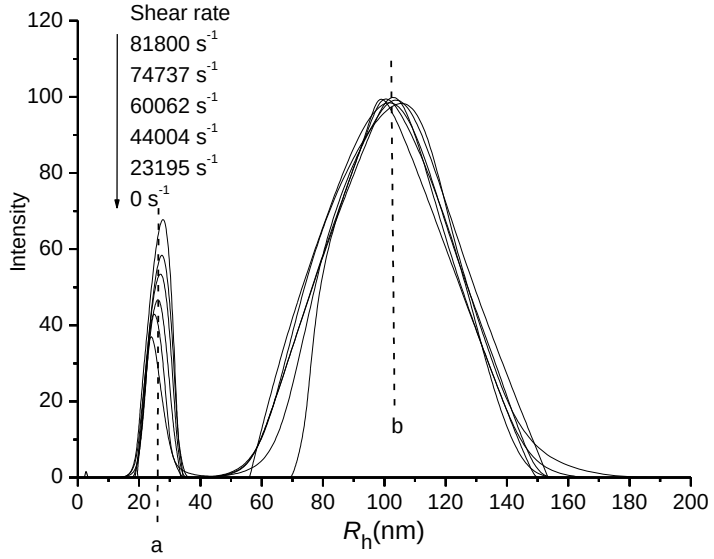


**Fig. 9.** Distributions of $R_h$ of PEI10000-HPAM in 1.0% NaCl aqueous solution after scission experiment with different shear rate in 1.0% NaCl aqueous solution.

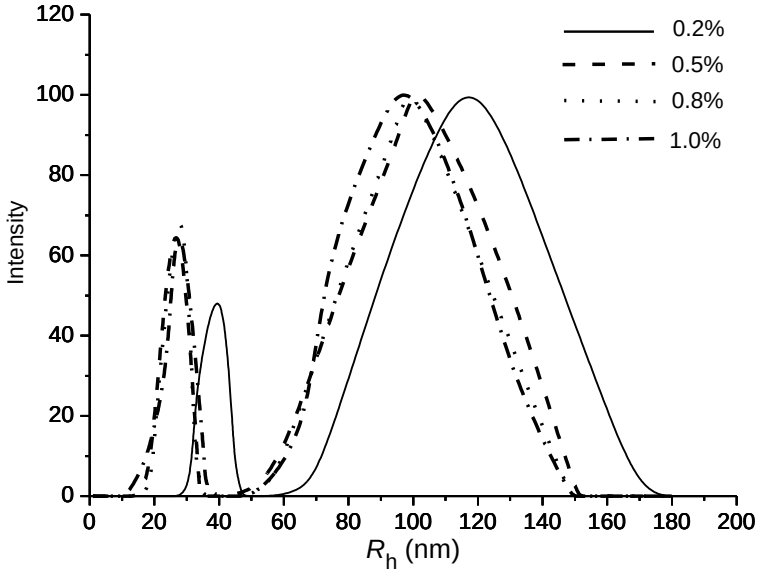


**Fig. 10.** Distributions of $R_h$ of PEI10000-HPAM in1.0% NaCl aqueous solution after scission experiment in different NaCl aqueous solution (shear rate ≈ 80,000$s^{-1}$).

## Conclusions

We report here an experimental study of flow-induced scission behaviour of star HPMAs with different numbers of arms in planar elongational flow that was conducted in distilled water and NaCl aqueous solutions in a cross-slot flow cell. It was found that the shear stability of linear and star HPAM had no difference in water without NaCl; no polymer chain scission (shear rate=20,000-100,000$s^{-1}$) was observed in both due to the strong polyelectrolyte behaviour of HPAM in water. However, in NaCl aqueous solutions ($C_{NaCl}$=0.2-1.0%wt), the star HPAMs exhibited

better shear stability than linear HPAM at the same shear rate, and the initial reduction rate of relative viscosity (*R*) decreased with the degree of branching of the HPAM. The initial rate of *R* of the five HPAMs exhibited an exponential dependence on shear rate in NaCl aqueous solutions, and the coefficient $C_1$ can be used to predict the shear stability of polymer viscosity. The increase of *R* of different star HPAMs with the shear rate in NaCl aqueous solutions can be attributed to the decrease in $R_h$ of HPAMs, while the increase of *R* with NaCl concentration may be due to the decrease in polymer viscosity $\eta_r$ as NaCl concentration increased.

## Experimental

### *Materials*

Poly(ethylene imine) (PEI 600, PEI 1800, PEI 3000 and PEI 10000, where 600, 1800, 3000 and 10000 are the weight-average molecular weight of the PEIs, respectively) was purchased from Aldrich. 2-Acetoxy thioxanthone [15] and 2-(2, 3-epoxy) propoxyl-thioxanthone [16] were synthesized according to literature procedures. Other chemicals were of analytical grade except as noted.

### *Preparation of Star PAM using PEI as the core (PEI-PAM)*

The synthetic route to PEI-PAMs is shown in Figure11. Thioxanthone-terminated PEIs were synthesized according to Ref [10]; they were used as the macrophotoinitiators. Photopolymerization of acrylamide (AM) was performed in a rectangular beaker by irradiating about 20 mL of 25wt% AM water solution at 40 °C in the presence of various thioxanthone-terminated PEIs.

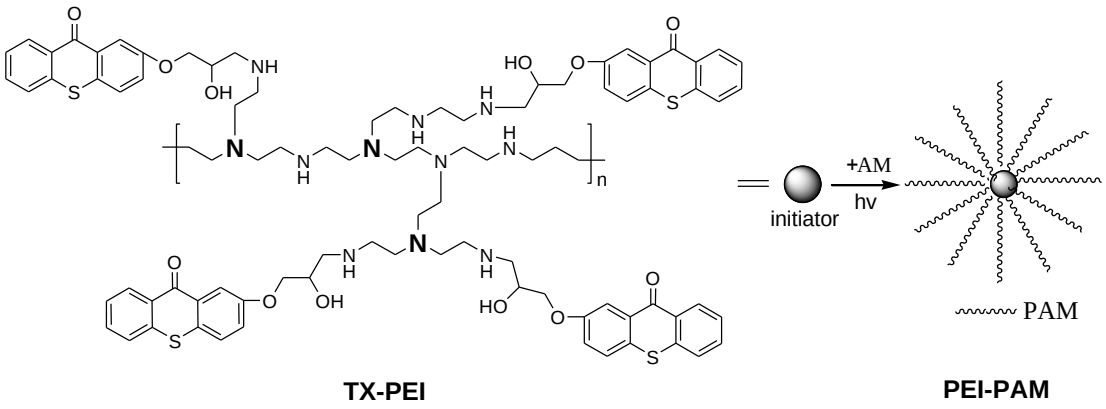


**Fig. 11.** Synthetic route to PEI-PAMs.

It was very difficult to investigate the number of arms of these star PAMs because, compared with the regular star polystyrene (PS) and poly(methyl methacrylate) (PMMA), star PAMs have much higher molecular weight and more flexible polymer chains [17]. As shown in Figure 12, we have confirmed the star structure of HPAM by atomic force microscope (AFM) [18]. Unfortunately, we cannot make sure the number of arms of these star PAMs because the number of arms of different macromolecules was not same. On the other hand, because of this result we also cannot estimate the difference between star PAMs before and after the shear degradation in terms of number of arms.

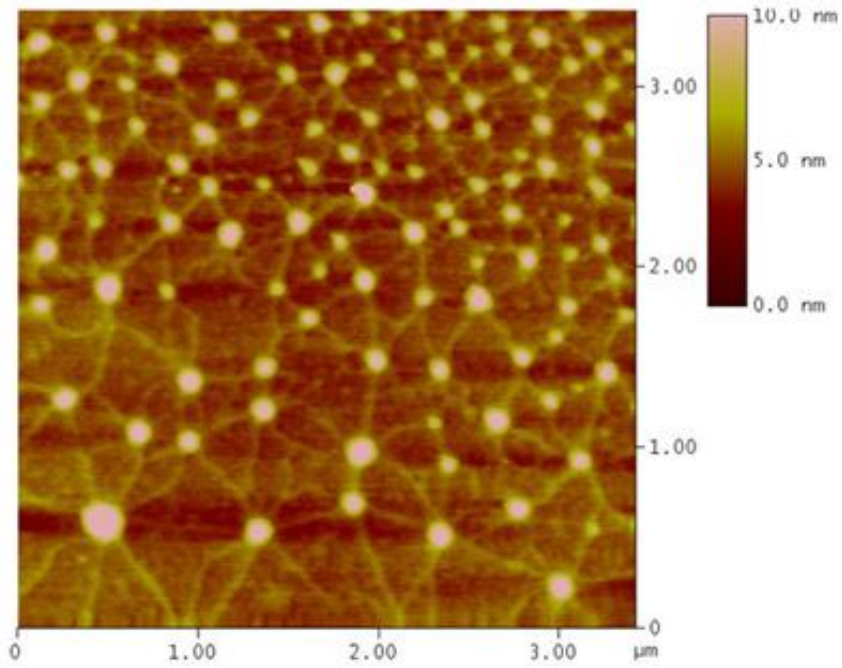


**Fig. 12.** AFM image of Star HPAM.

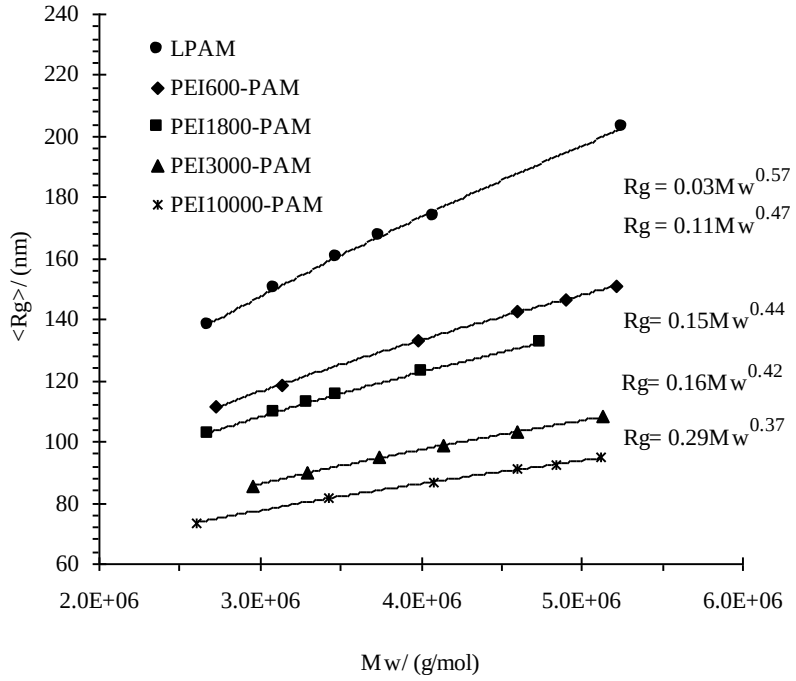


**Fig. 13.** The relationships of radius of gyration ($R_g$) and molecular weight ($M_w$) for LPAM and PEI-PAMs.

The branching index ($g$) factor has usually been used to investigate the content of branching for long, flexible polymer chains. The number of arms of a star polymer increases with the decrease of the value of $g$ [17, 19, 20]. The relationships of radius of gyration ($R_g$) and molecular weight ($M_w$) for LPAM and PEI-PAMs are shown in Figure 13. The branching index ($g$) factor, which is defined as the ratio of the mean square radius of gyration of a branched polymer to that of a linear one at the same

molecular weight, was used to characterize the degree of branching of the polymer [19].

$$g \equiv \left(\frac{< R_g^2 >_b}{< R_g^2 >_l}\right)_M \quad (3)$$

where the subscripts *b* and *l* represent the branched and linear polymer, respectively.

Five samples, with similar $M_w$, were chosen to study their shear degradation resistances during elongational flow; their molecular characteristics are reported in Table 5. It is assumed the number of branches increase (branch length decrease) with increasing PEI molecular weight.

**Tab. 5.** Some data for the five PAMs.

| Sample | LPAM | PEI600-PAM | PEI1800-PAM | PEI3000-PAM | PEI1000-PAM |
|---|---|---|---|---|---|
| $M_w/10^6$(SLS) | 4.08 | 3.98 | 4.01 | 4.14 | 4.08 |
| $R_g$(nm) | 174.1 | 133.0 | 122.9 | 98.9 | 87.0 |
| *g* | 1 | 0.77 | 0.70 | 0.55 | 0.49 |
| [η](dL/g) | 9.30 | 9.03 | 8.84 | 8.72 | 8.63 |

### *Preparation of Star HPAM using PEI as the core (PEI-HPAM)*

Star PAM (6g) was dissolved in water (20mL). NaOH solution (4.9%wt, 20 mL) was added to the PAM solution and the hydrolysis reaction was allowed to proceed, without stirring, at 40 °C for 12 h and the reaction mixture was then precipitated in excess ethanol. After being collected by filtration, the polymer was kept in a vacuum oven for drying. The degree of hydrolysis of these star PEI-HPAMs was determined by the titration method and their molecular characteristics are shown in Table 6.

**Tab. 6.** Some data for the five HPAMs.

| Sample | LHPAM | PEI600-HPAM | PEI1800-HPAM | PEI3000-HPAM | PEI1000-HPAM |
|---|---|---|---|---|---|
| [η](dL/g) | 12.90 | 11.91 | 11.46 | 11.03 | 10.28 |
| Degree of hydrolysis (%) | 30.1 | 30.0 | 29.9 | 30.1 | 30.1 |

### *Solution Preparation for Flow-Induced Scission Experiments*

Solutions were prepared by a weighing method. Stock solutions with the same concentration of 1500mg/L in NaCl aqueous solution ($C_{NaCl}$=0.2-1.0%wt) for linear HPAM (LHPAM) and PEI-HPAM were directly prepared form the dry samples. The stock solution was kept in a 500 mL volumetric flask, which was rotated using a slow speed motor to make the stock solution uniform.

### *Cross-Slot Flow Cell*

Odell [11] invented a cross slot device to study the flow-induced chain fracture of isolated linear macromolecules in solution in 1986. Recently, Xue et al [14] made some changes to make it more operable; a schematic representation of this device is shown in Fig. 14. As shown in Figure 14a, the cross-slot flow cell was made according to the Ref [14]. Figure 14b shows the plane view of the central block with a

cross-slot of width *d*=0.3mm and depth *l*=2.5mm. The approach length to the slot was 4 mm.

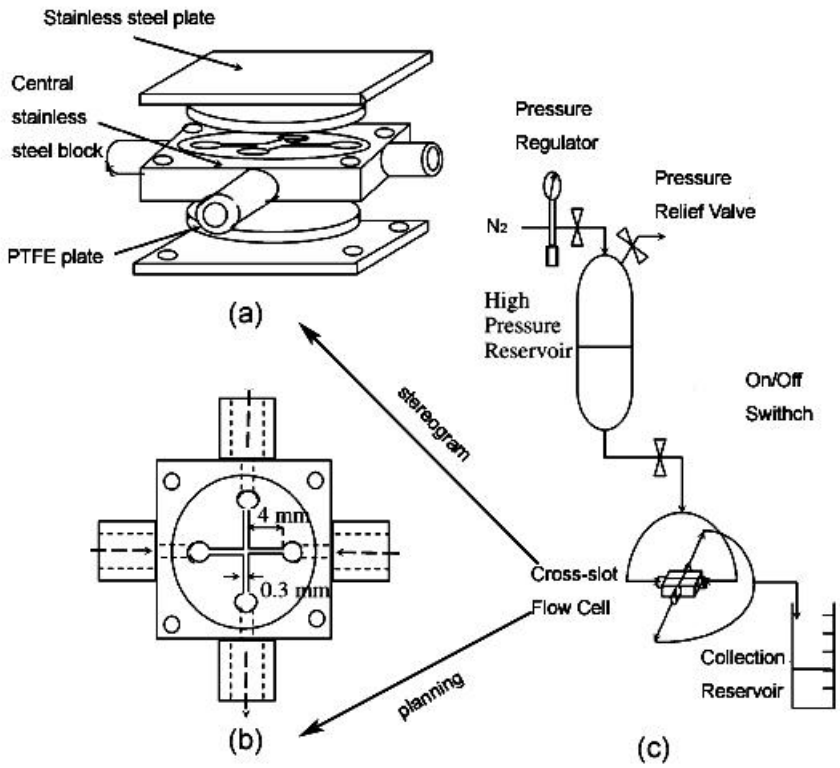


**Fig. 14.** Schematic of (a) the construction of the cross-slot flow cell (b) the top view of the central block, and (c) the flow arrangements for high strain rate experiments.

### *Flow-Induced Scission Experiments*

The high-pressure flow arrangement used for the high strain rate experiments is shown in Figure 14c. The star PEI-PAMs solution (300 mL) was filled into the high-pressure reservoir. For a desired volumetric flow rate (Q), a regulated nitrogen gas pressure (0-2M pa) was applied to the reservoir. The solution was led through two opposing slots, to the collection reservoir. Q was determined from the measured flow time. The nominal extensional shear rate ($\dot{\varepsilon}$) was estimated as $\dot{\varepsilon}=Q/d^2l$ [11]. In this paper, 20,000<$\dot{\varepsilon}$<100,000 $s^{-1}$. Samples (20 mL each) were withdrawn from the collection reservoir to measure the relative viscosity ($\eta_r$) immediately after the scission experiment by using an Ubbelohde viscometer at 30 °C. The reduction degree of $\eta_r$ ($\Delta\eta_r$) was estimated as $\Delta\eta_r=(\eta_{r,b}-\eta_{r,a})/\eta_{r,b}$, $\eta_{r,b}$ and $\eta_{r,a}$ are the $\eta_r$ of the polymer solution before and after high-pressure flow, respectively. The initial rate of reduction of relative viscosity (*R*) at different strain rates was estimated from $\Delta\eta_r$ and the corresponding number of passes (*n*): $R=\Delta\eta_r Q/n\,d^2l$[14], in this paper *n*=3.

Intrinsic viscosities ($[\eta]$) of the polymers withdrawn from the reservoir were measured with the “five-spot” dilution method method using an Ubbelohde viscometer at 30 °C. The solvent used was 0.1 mol/L NaCl aqueous solution. The reduction rate of $[\eta]$ ($\Delta[\eta]$) was estimated as $\Delta[\eta]=([\eta]_b-[\eta]_a)/[\eta]_b$, $[\eta]_b$ and $[\eta]_a$ are the $[\eta]$ of the polymer solution before and after high-pressure flow, respectively.

### *Solution Preparation for Dynamic Light Scattering*

After the elongation flow-induced scission experiments, the samples (25 mL) which were withdrawn from the collection reservoir were kept in a 40 °C water bath for at least 4 days, and then the stock solution was stirred slowly by rotating the volumetric flask at slow speed for at least another 2 days.

### *Static Light Scattering (SLS)*

The light scattering instrument employed was a BI-200SM multiangle laser light scattering detector purchased from Brookheaven Instrument Corp., operating at 532 nm. The BI-200SM detector was calibrated with toluene and Rayleigh ratio of toluene is $2.803 \times 10^{-5}$ $cm^{-1}$. The dn/dc value for PAM in 0.1mol/L NaCl at 25 °C is 0.1700 mL/g. Data were collected and processed by Berry Plot Software Ver. 3.41 (Brookheaven Instrument Corp.). The weight average molecular weight ($M_w$) and radius of gyration ($R_g$) reported in this paper were based on the double extrapolation method of Berry ($(Kc/R_\theta)^{1/2}$ vs $\sin^2(\theta/2) + kc$).

### *Dynamic Light Scattering (DLS)*

A Brookhaven Instruments BI-200SM goniometer and a BI-9000 correlator were used to measure the intensity-intensity autocorrelation functions for vertically polarized $\lambda_0$=532 nm light scattered from clarified polymer solutions at $90^0$.

Hydrodynamic radius ($R_h$) was investigated by the DLS and calculated according to the CONTIN algorithm. The change of $R_h$ can reflect the change of molecule weight of the polymer. Under the same conditions, $R_h$ increases with the molecule weight and the $\eta_r$ increases with the $R_h$.

### *Acknowledgements*

This work is financially supported by The Key Technologies R&D Program of China (No. 2008ZX05024-002) and State Key Laboratory of Oil/Gas Reservoir Geology and Exploitation, China (No. PLN-ZL004).

## References

[1] Durst, F.; Haas, R.; Kaczmar, B.U. *J. Appl. Polym. Sci.***1981**, *26, 3125*.
[2] Wang, D.M.; Jiang, Y.L.; Wang, Y. *SPE 77496*, **2002**: *1*.
[3] Xu, G.L.; Sun, G.; Shao, Z.B. *Oilfield Chemistry* **2006**, *23,341*. (in Chinese)
[4] Ma, H.W.; Shan, J.; Shen, X. L. *China Petroleum Machinery***2005**, *33, 33*. (in Chinese)
[5] Qian, S.P. *China University of Geosciences* (Beijing) 2006. (in Chinese).
[6] Barnard, B.J.S.; Sellin, R.H.J. *Nature Phys. Sci.***1972**, *236,12*.
[7] Kim, O.K.; Little, R.C.; Patterson, R.L. *Nature***1974**, *250, 408.*
[8] Agarwal, S.H.; Jenkins, R.F.; Porter, R.S. *J. App. Polym. Sci.***1982**, 27, 113.
[9] Ungeheuer, S.; Bewersdorff, H.W.; Singh, R.P. *J. Appl. Polym. Sci.***1989**, *37, 2933.*
[10] Fang, S.W.; Duan, M.; Jiang, C.Y. *J. Macromol. Sci. Part A: Pure. Appl. Chem.* **2010,** *47,49.*
[11] Odell, J.A.; Keller, A.; Wills, H. H. *J Polym. Sci. Polym. Phys.***1986,** *24, 1889.*
[12] Islam, M.T.; Vanapalli, S.A.; Solomon, M.J. *Macromolecules* **2004**, *37, 1023.*

[13] Buchholz, B.A.; Zahn, J.M.; Kenward, M.; Slater, G.W.; Barron, A.E. *Polymer* ***2004****, 45, 1223.*
[14] Xue, L.; Agarwal, U. S.; Lemstra, P. J. *Macromolecules* **2005**, *38, 8825.*
[15] Catalina, F.; Tercero, J.M.; Peinado, C.; Sastre, R.; Mateo, J.L. *J Photochem. Photobiol. A: Chem.***1989**, *50,,249.*
[16] Yang, J. W.; Zeng, Z. H.; Chen, Y. L. *J Polym. Sci. Part A: Polym. Chem.***1998**, *36,2563.*
[17] Hirao, A.; Watanabe, T. *Macromolecules* **2009**, *42, 682*.
[18] Fang, S. W.; Duan, M.; Jiang, C. Y.; Zhang, J. *Petrochemical Technology* **2009**, *38, 278.(In Chinese)*
[19] Yu, Y.L.; DesLauriers, P.J.; Rohlfing, D. C. *Polymer* **2005**, *46, 5165.*
[20] Grcev, S.; Schoenmakers, P.; Iedema, P. *Polymer* **2004**, *45, 39.*